iScience

CellPress
OPEN ACCESS

Article

Roseburia intestinalis relieves intrahepatic cholestasis of pregnancy through bile acid/FXR-FGF15 in rats

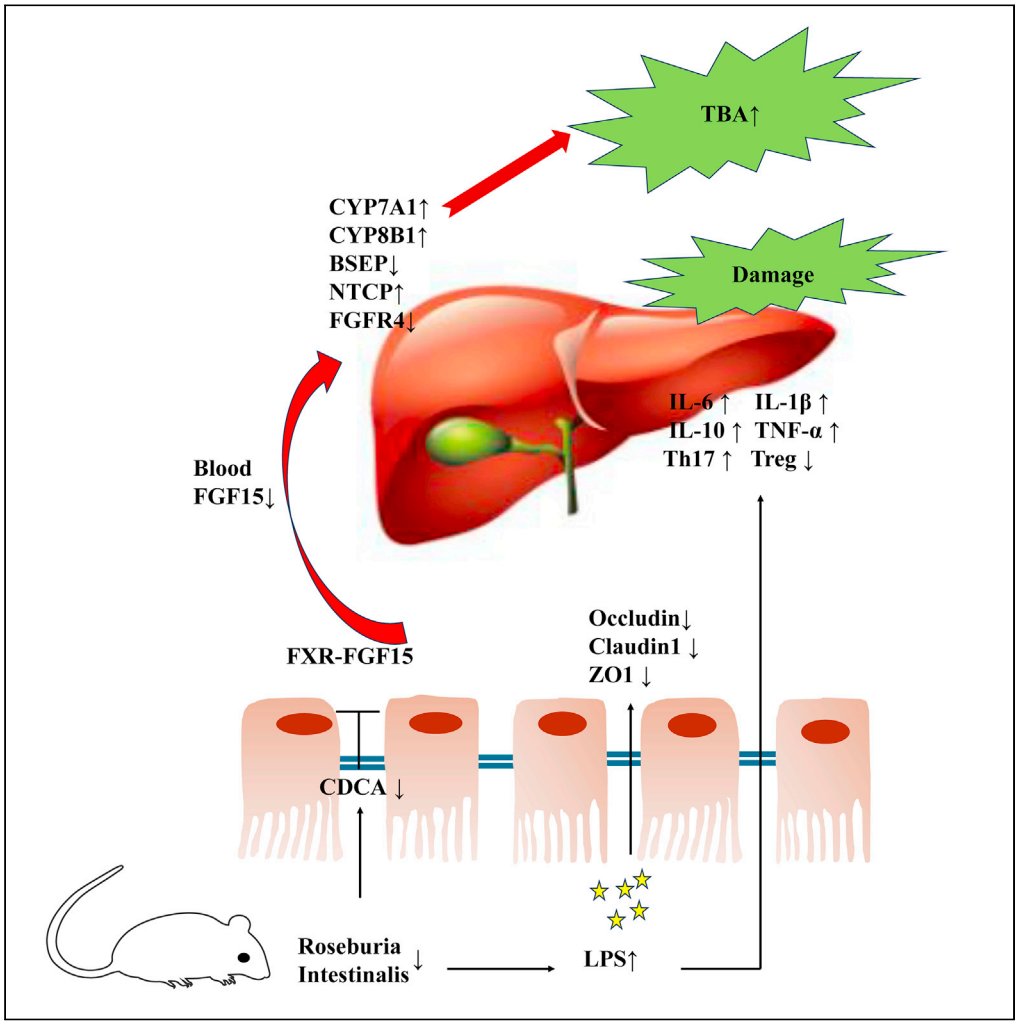

Hanxiang Sun, Xiujuan Su, Yang Liu, Guohua Li, Qiaoling Du

19921781186@139.com

Highlights

Roseburia intestinalis (R.I) is the key bacteria in ICP

R.I. improved phenotypes associated with ICP through bile acid/FXR-FGF15 pathway

Roseburia intestinalis may be a promising target for the treatment of ICP

Sun et al., iScience *26*, 108392
December 15, 2023
https://doi.org/10.1016/j.isci.2023.108392

iScience

CellPress
OPEN ACCESS

Article

Roseburia intestinalis relieves intrahepatic cholestasis of pregnancy through bile acid/FXR-FGF15 in rats

Hanxiang Sun,[1] Xiujuan Su,[2] Yang Liu,[1] Guohua Li,[3] and Qiaoling Du[1,4,*]

SUMMARY

Previous research has demonstrated significant differences in intestinal flora between pregnant women with intrahepatic cholestasis of pregnancy (ICP) and healthy pregnant women. The objective of our study is to identify the key bacteria involved in ICP rats and explore the underlying mechanism. We established an ICP rat model and collected rat feces for metagenomic sequencing and found that *Roseburia intestinalis* (R.I) is the key bacteria in ICP. Transplantation of R.I improved phenotypes associated with ICP through the bile acid/farnesoid X receptor-fibroblast growth factor 15 (FXR-FGF15) signaling pathway. We used the FXR antagonist Z-Guggulsterone (Z-Gu) to verify the key role of FXR in ICP and found that Z-Gu reversed the benefits of R.I on ICP rats. Our research highlights the important role of intestinal flora in the pathogenesis of ICP and provides a novel approach for its treatment.

INTRODUCTION

Intrahepatic cholestasis of pregnancy (ICP) is a pregnancy complication characterized by skin pruritus, jaundice, elevated serum bile acid, and abnormal liver enzymes.[1] Its clinical incidence is as high as 2%–4%,[2] mostly occurring in the third trimester of pregnancy. Although most discomfort symptoms of pregnant women are relieved 2 to 3 weeks after delivery, ICP can cause poor prognosis,[3] such as premature delivery (19%–60%), fetal distress (22%–33%), and even fetal death (1%–2%). The perinatal mortality rate is about 6–10 times higher than that of normal pregnancy.[1] Many studies have shown that the concentration of serum bile acid in ICP pregnant women is positively correlated with intrauterine complications such as fetal death.[4] Every 1 μm mol/L increase in serum bile acid of pregnant women increases the risk of spontaneous preterm delivery, fetal asphyxia, or meconium contamination of the amniotic fluid by 1%–2%.[5] When the serum bile acid of pregnant women is more than 100 μm mol/L, the risk of fetal stillbirth increases 10-fold.[6] Therefore, ICP seriously endangers maternal and infant health.

The human intestinal tract is a crucial site for bacterial colonization.[7] Bile acid is synthesized and conjugated by cholesterol in the liver, then secreted into the intestine, and is metabolized and transformed by intestinal microflora through uncoupling, dihydroxylation, and other reactions.[8] Farnesoid X receptor (FXR) is highly expressed in the gastrointestinal tract, which inhibits bile acid synthesis.[9,10] FXR is considered to be activated by endogenous ligands such as chenodeoxycholic acid (CDCA) and antagonized by taurine-β-mouse cholic acid (T-β-MCA).[11–16]

FXR plays a vital role in regulating the enterohepatic circulation of bile acid by affecting its synthesis and transport, thus maintaining bile acid balance.[17] Cytochrome P450 family 7 subfamily A member 1 (CYP7A1) is a key enzyme in bile acid synthesis. In the liver, FXR inhibits bile acid synthesis by reducing the expression of CYP7A1 and cytochrome P450 family 8 subfamily B member 1 (CYP8B1), thus playing a prominent role in bile acid synthesis through small heterodimer partner (SHP).[18,19] Cytochrome P450 family 7 subfamily B member 1 (CYP7B1) and sterol 27-hydroxylase (CYP27A1) are two other important enzymes in bile acid synthesis. Fibroblast growth factor 15 (FGF15) is a hormone secreted into the portal vein that inhibits the expression of CYP7A1 in the liver.[20] Intestinal FXR can induce FGF15, which activates liver fibroblast growth factor receptor 4 (FGFR4) and ultimately inhibits the expression of CYP7A1 and CYP8B1.[10] FXR can also increase the expression of bile salt export pump (BSEP) and inhibit the expression of sodium taurocholate cotransporting polypeptide (NTCP) to maintain a low level of bile acid in hepatocytes and prevent cholestatic liver injury.[21,22] Therefore, liver FXR and intestinal FXR jointly regulate bile acid synthesis and transport.

Roseburia intestinalis (R.I) is a gram-positive anaerobic bacterium that produces butyric acid and belongs to the phylum Firmicutes. It functions through intermediate metabolites such as butyric acid, supernatant, and flagellin.[23,24] Studies have shown that R.I can play a therapeutic role in inflammatory bowel disease, atherosclerosis, alcoholic fatty liver, colorectal cancer, and metabolic syndrome by regulating intestinal

[1]Department of Obstetrics, Shanghai Key Laboratory of Maternal Fetal Medicine, Shanghai First Maternity and Infant Hospital, School of Medicine, Tongji University, Shanghai 200092, China
[2]Clinical Research Center, Shanghai Key Laboratory of Maternal Fetal Medicine, Shanghai First Maternity and Infant Hospital, School of Medicine, Tongji University, Shanghai 200092, China
[3]Department of Reproductive Immunology, Shanghai Key Laboratory of Maternal Fetal Medicine, Shanghai First Maternity and Infant Hospital, School of Medicine, Tongji University, Shanghai 200092, China
[4]Lead contact
*Correspondence: 19921781186@139.com
https://doi.org/10.1016/j.isci.2023.108392

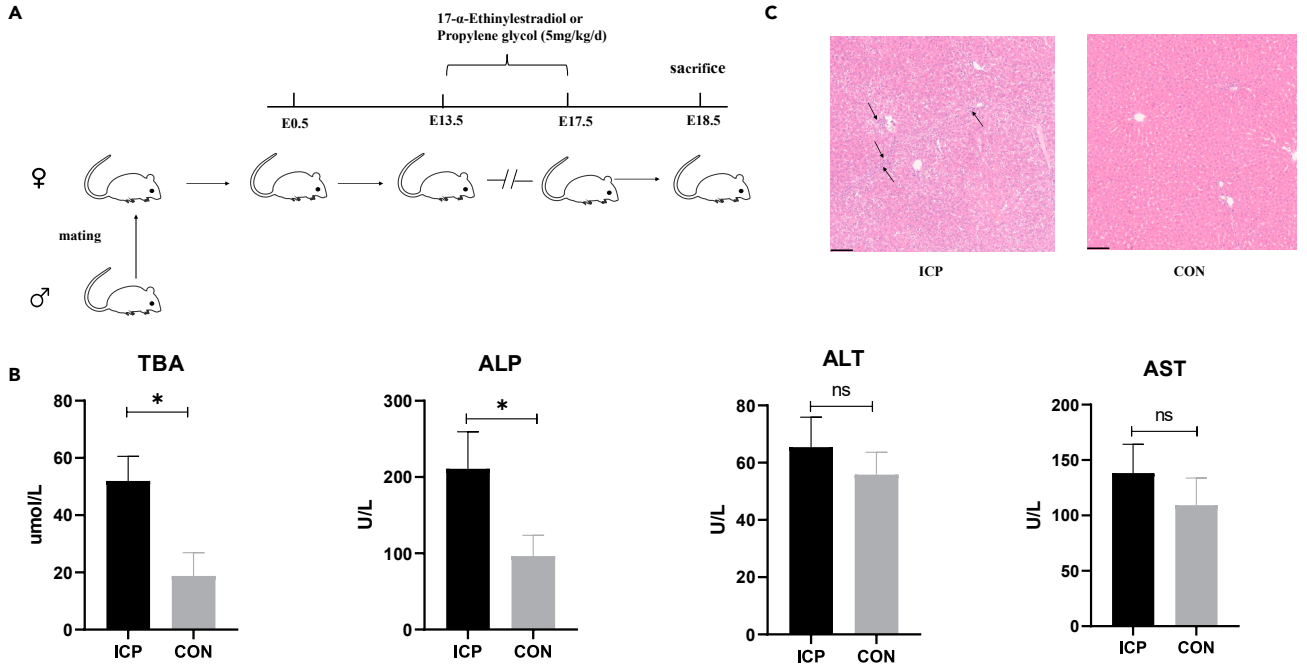

Figure 1. Estrogen-induced cholestasis of pregnancy in rats showed elevated serum bile acids and liver damage

(A) An experimental design: Male and female rats were mated, and female rats were injected with 17-α- ethinyl estradiol subcutaneously every day from day 13.5 to day 17.5 after pregnancy to establish ICP pregnancy model rats.

(B) TBA, ALP, ALT, and AST levels in the serum.

(C) Representative H&E staining of the liver tissues (original magnification 100×). Scale bars, 100 μm. Data are represented as mean ± SEM, n = 6. *p < 0.05, ns represents no statistical significance. The arrow refers to the infiltration of inflammatory cells.

barrier homeostasis, intestinal immune cells, and releasing cytokines through metabolites such as butyric acid and flagellin. It is a potential "next-generation probiotic."[25–27] However, whether R.I can alleviate ICP has not been reported.

Recent studies have indicated significant differences in intestinal microflora between pregnant women with ICP and healthy pregnant women,[28,29] suggesting an association between ICP and intestinal microflora. However, the key microbial and host targets associated with ICP remain unknown. Our study has revealed that the transplantation of feces from ICP model rats to pseudo-germfree healthy pregnant rats resulted in an increase in blood bile acid levels and pathological changes in the liver. This indicated that an imbalance in the intestinal flora is one of the causes of ICP. To identify the specific bacteria involved, we analyzed the correlation between serum total bile acids and alkaline phosphatase (ALP) levels, as well as the results of metagenomic analysis. Our findings suggest that R.I may play a significant role in the development of ICP. Our research further demonstrated that R.I is affected by bile acid synthesis and transport through the bile acid/FXR-FGF15 pathway, thereby alleviating cholestasis in ICP rats. Moreover, our findings suggests that R.I can prevent the leakage of lipopolysaccharide (LPS) from the intestine, repair intestinal barrier function, and decrease liver inflammation and improve immune imbalance.

RESULTS

Estrogen-induced cholestasis of pregnancy in rats showed elevated serum bile acids and liver damage

To begin with, the ICP rat model was established through subcutaneous injection of 17-α-ethinylestradiol for five consecutive days. The control group, on the other hand, was subcutaneously injected with (±)-1,2-Propanediol (Figure 1A). The cholestasis induced by estrogen led to a significant increase in serum total bile acid (TBA) and ALP levels (Figure 1B). Although the serum glutamic-pyruvic transaminase (ALT) and glutamic oxaloacetic transaminase (AST) of rats in ICP group were higher than those in control group, we did not observe a significant statistical difference between the two groups (Figure 1B). Furthermore, liver hematoxylin and eosin (H&E) staining revealed hepatocyte necrosis and inflammatory infiltration in the liver of rats with cholestasis (Figure 1C).

Rats with estrogen-induced ICP exhibited abnormalities in intestinal barrier function, liver inflammation, T cell immunity, bile acid synthesis, and transporters

Estrogen-induced cholestasis during pregnancy resulted in an increase in serum LPS levels (Figure 2A). Immunohistochemical examination of intestinal barrier proteins, including Occludin, Claudin1, and tight junction protein 1 (ZO1), revealed a decrease in their expression in the colon of ICP rats (Figure 2D). This suggested that estrogen-induced cholestasis during pregnancy can reduce intestinal barrier function. We also evaluated liver inflammation and T cell immunity and found that messenger RNA (mRNA) levels of liver inflammatory factors, including

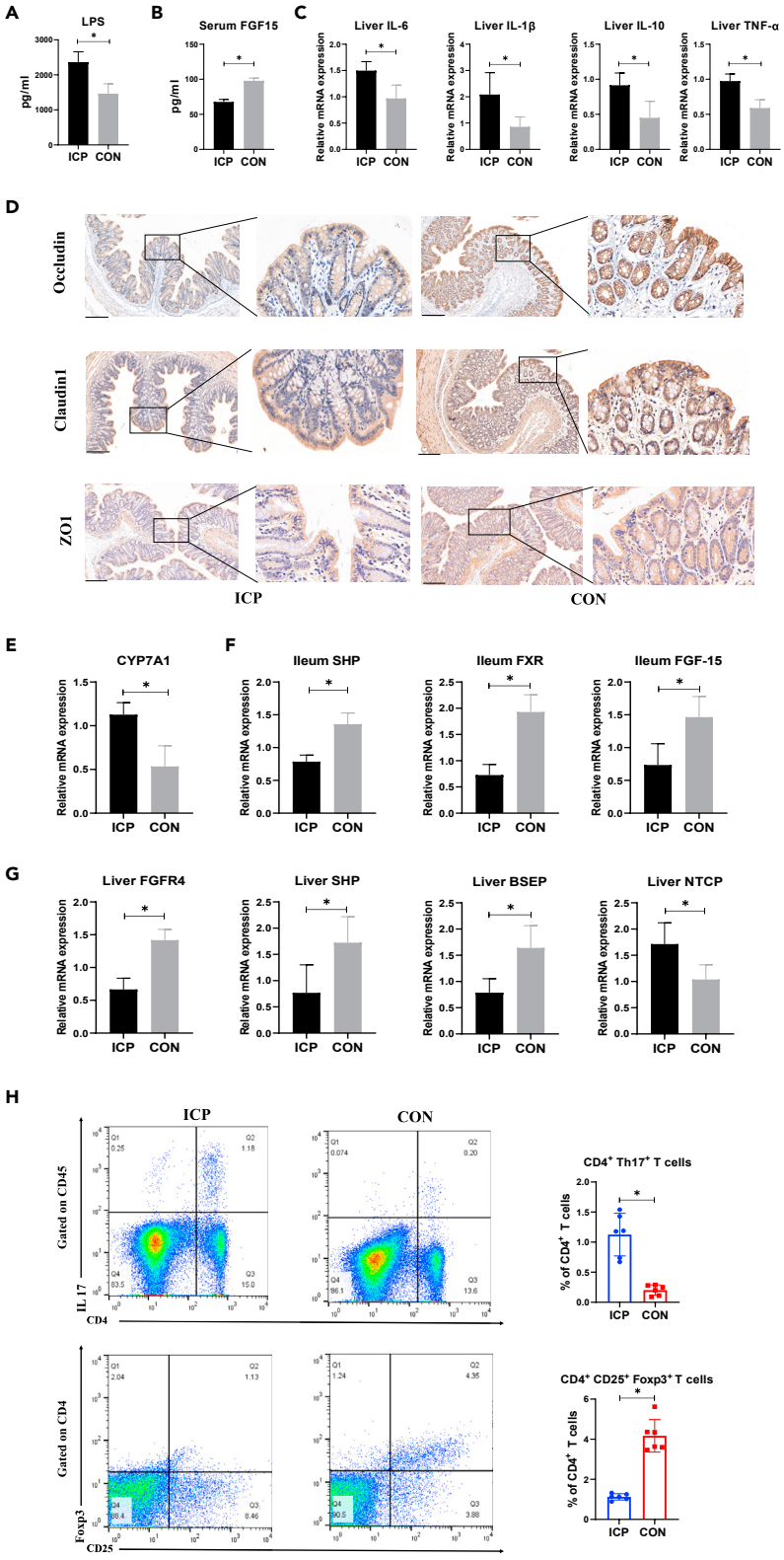

Figure 2. Intestinal barrier function, liver inflammation, and T cell immunity, bile acid synthase, and transporter were abnormal in rats with estrogen-induced cholestasis of pregnancy

(A) Serum LPS level.

Figure 2. *Continued*
(B) Serum FGF15 level.
(C) Hepatic mRNA expression of IL-6, IL-1β, IL-10, and TNF-α.
(D) Immunohistochemistry staining for Occludin, Claudin1, and ZO1 in the colon in ICP rats and control rats was tested. The magnification is 100× and 400×, respectively. Scale bars, 100 μm.
(E) mRNA expression of CYP7A1 in the liver.
(F) mRNA expression of SHP, FXR, and FGF15 in the ileum.
(G) mRNA expression of FGFR4, SHP, BSEP, and NTCP in the liver.
(H) The representative flow cytometric plots of $CD4^+CD25^+Foxp3^+$ Treg and $CD4^+IL\text{-}17^+$ Th17 cells, respectively; and proportions of Th17 and Treg cells in each group. Data are presented as means ± SD, n = 6. *p < 0.05, CON, control group; ICP, model group.

interleukin-6 (IL-6), interleukin-1β (IL-1β), interleukin-10 (IL-10), and tumor necrosis factor α (TNF-α), significantly increased in the liver of ICP rats (Figure 2C). Furthermore, T helper cell 17 (Th17) in the liver of ICP rats significantly increased, while regulatory T cell (Treg) significantly decreased (Figure 2H). Additionally, we tested the mRNA levels of bile acid synthase and bile acid transporter in ICP rats and found that the mRNA levels of liver bile acid synthesis rate-limiting enzyme CYP7A1 significantly increased, and the protein level of CYP7A1 and CYP8B1 also significantly increased (Figure S1B). But CYP7B1 and CYP27A1 did not change (Figure S1A). The mRNA levels of FGFR4, SHP, and BSEP in the liver decreased, while NTCP increased, and the mRNA levels of SHP, FXR, and FGF15 in the ileum decreased (Figures 2E–2G). Moreover, the protein level of FXR and FGF15 also significantly decreased (Figure S1B). Additionally, serum FGF15 in ICP rats significantly decreased (Figure 2B). These results indicated that the synthesis and transport of bile acids in ICP rats were affected, and the FXR-FGF15 signal pathway was inhibited.

Estrogen-induced cholestasis during pregnancy in rats associates with gut microbiota dysbiosis and compositional changes in the bile acid pool

In order to investigate the changes in intestinal microorganisms between ICP rats and control rats of the same gestational age, we collected fecal samples from both groups at 18.5 days of pregnancy for metagenomic sequencing. Our results showed that the biodiversity of intestinal microorganisms in ICP rats was significantly reduced compared to the control group, as indicated by the Shannon index (Figure 3A). Principal coordinates analysis (PCoA) revealed significant differences in the composition of intestinal microflora between ICP rats and the control (CON) group (Figure 3B). We also analyzed the dominant species composition of both groups at the species level (Figure 3C) and identified bacterial species with significant differences between the two groups using the Mann-Whitney U test ($p < 0.05$) (Figure 3D). We also showed the heatmap of 50 Kyoto Encyclopedia of Genes and Genomes (KEGG)_pathways with the highest abundance in the supplemental information (Figure S2). Additionally, we measured targeted bile acids in the fecal samples and found that the fecal CDCA levels were significantly lower in ICP rats compared to the CON group (Figure 3E), with significant differences observed in other types of bile acids as well (Figure S3A). Our study highlights significant differences in intestinal microorganisms and bile acids between ICP rats and control rats of the same gestational age.

Fecal microflora from ICP model rats aggravated liver injury and increased serum bile acid and ALP levels in pseudo-germfree rats

We collected fecal samples from both ICP model rats and control pregnant rats in advance and stored them in a refrigerator at −80°C for fecal microbiota transplantation (FMT). Female rats were administered quadruple antibiotics to cleanse their intestines between 1.5 and 6.5 days of pregnancy in order to establish pseudo-germfree rats. Fecal samples collected in advance from both ICP model rats and control pregnant rats were then transplanted into healthy pseudo-germfree pregnant rats between 7.5 and 17.5 days of pregnancy (referred to as FMT-ICP and FMT-CON, respectively) (Figure 4A). After sacrificing the rats at 18.5 days of pregnancy, it was discovered that the levels of serum bile acid and ALP in the FMT-ICP group were significantly higher than those in the FMT-CON group. However, there was no significant difference in ALT and AST between the two groups (Figure 4C). Liver H&E staining also indicated that hepatocyte necrosis and inflammatory infiltration in FMT-ICP rats were more severe than those in FMT-CON rats (Figure 4B). The aforementioned experimental results demonstrated that an imbalance in intestinal flora was one of the causes of ICP. Based on the macrogenome results of this animal experiment, combined with the previous 16S ribosomal RNA (16SrRNA) results of feces of pregnant women with ICP,[30] we screened three bacteria that may play a key role in ICP (*Roseburia intestinalis*, *Roseburia Hominis*, and *Faecalibacterium Prausnitzii*). We further analyzed the correlation between serum total bile acids and ALP of rats and species-level bacteria and speculated that R.I played an important role in ICP (Figure S3D). Next, we conducted animal experiments to verify whether R.I alleviated ICP in rats.

Transplantation of R.I reduced serum bile acid levels and mitigated liver injury in ICP rats

Different from the earlier FMT experiment requiring pseudo-aseptic treatment, transplantation of R.I and phosphate buffered solution (PBS) does not need pseudo-aseptic treatment. R.I and PBS were transplanted into pregnant rats with ICP between 7.5 and 17.5 days of gestation, while the CON group consisted of healthy pregnant rats without any treatment (Figure 5A). Upon sacrifice of the rats on the 18.5th day of gestation, it was observed that R.I transplantation resulted in a decrease in serum bile acid and ALP levels in ICP rats compared to PBS transplantation (Figure 5C), with no significant difference in ALT and AST levels. Moreover, we did not observe any statistical difference in serum indexes between the CON group and ICP+R.I group (Figure 5C). Furthermore, liver H&E staining of ICP rats after R.I transplantation showed

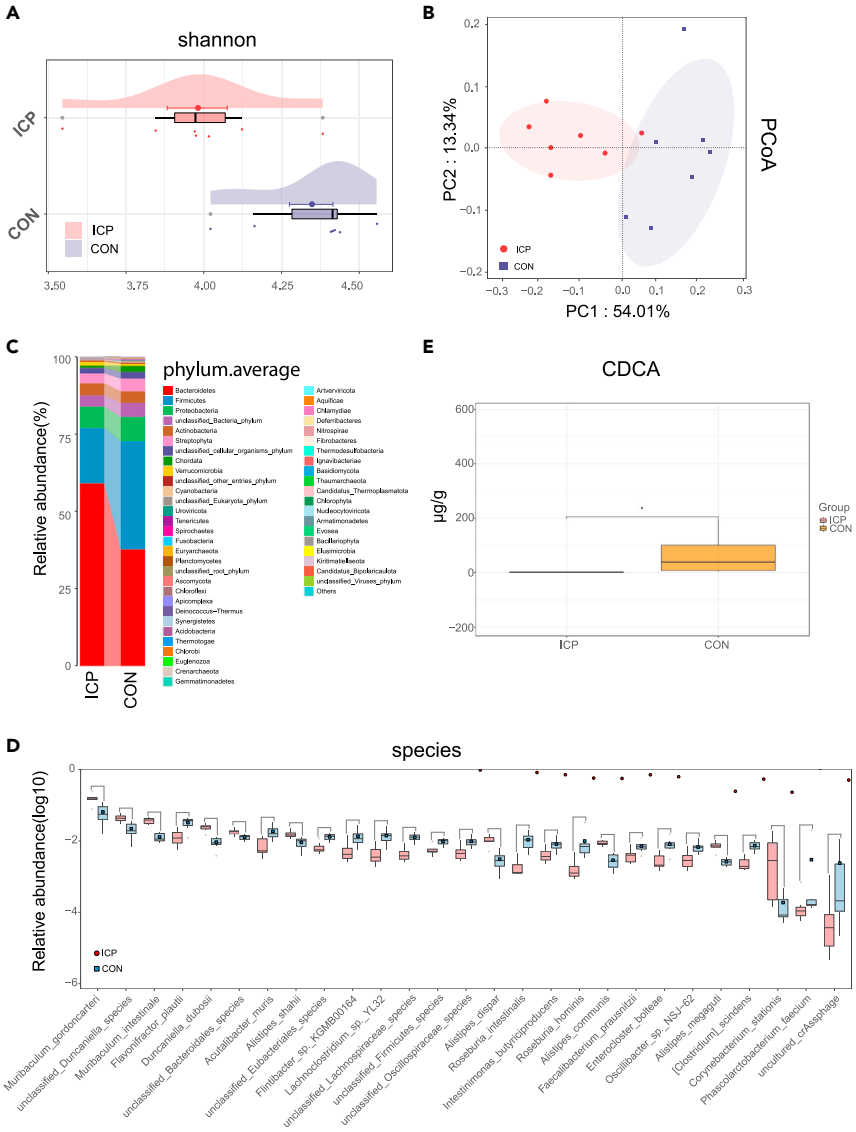

Figure 3. Estrogen-induced cholestasis during pregnancy in rats induced gut microbiota dysbiosis and bile acid dysbiosis

(A) α-diversity analysis between two groups using the Shannon index.

(B) Principal coordinates analysis (PCoA).

(C) Microbiota composition at the phylum level.

(D) Microbiota at the species levels with significant differences between the two groups was selected by the Mann-Whitney U test.

(E) Fecal levels of CDCA. Data are represented as mean ± SEM, n = 7.

an improvement in hepatic lobular structure disorder, hepatocyte necrosis, and inflammatory infiltration, significantly improving the pathological changes in the liver compared to PBS transplantation (Figure 5B). Additionally, fecal CDCA levels significantly increased in ICP rats after R.I transplantation (Figure 5D), with significant differences observed in other types of bile acids as well (Figure S3B).

R.I transplantation ameliorated the pathological phenotype of ICP rats and activated the FXR-FGF15 signaling pathway

The transplantation of R.I significantly reduced serum LPS levels in ICP rats (Figure 6A). We assessed intestinal barrier-related proteins using immunohistochemistry. Our findings indicate that Occludin, Claudin1, and ZO1 levels increased significantly after R.I transplantation (Figure 6D), suggesting that R.I transplantation restored intestinal barrier function. Additionally, R.I transplantation mitigated the increase in liver inflammatory factors IL-6, IL-1β, IL-10, and TNF-α induced by ICP (Figure 6C). R.I transplantation also reduced Th17 and increased Treg in the liver of ICP rats (Figure 6H). Importantly, compared to PBS transplantation, R.I transplantation improved bile acid synthesis and transport, including decreased mRNA and protein levels of CYP7A1 and CYP8B1 in the liver (Figure 6E; Figure S4B), but no change in mRNA expression

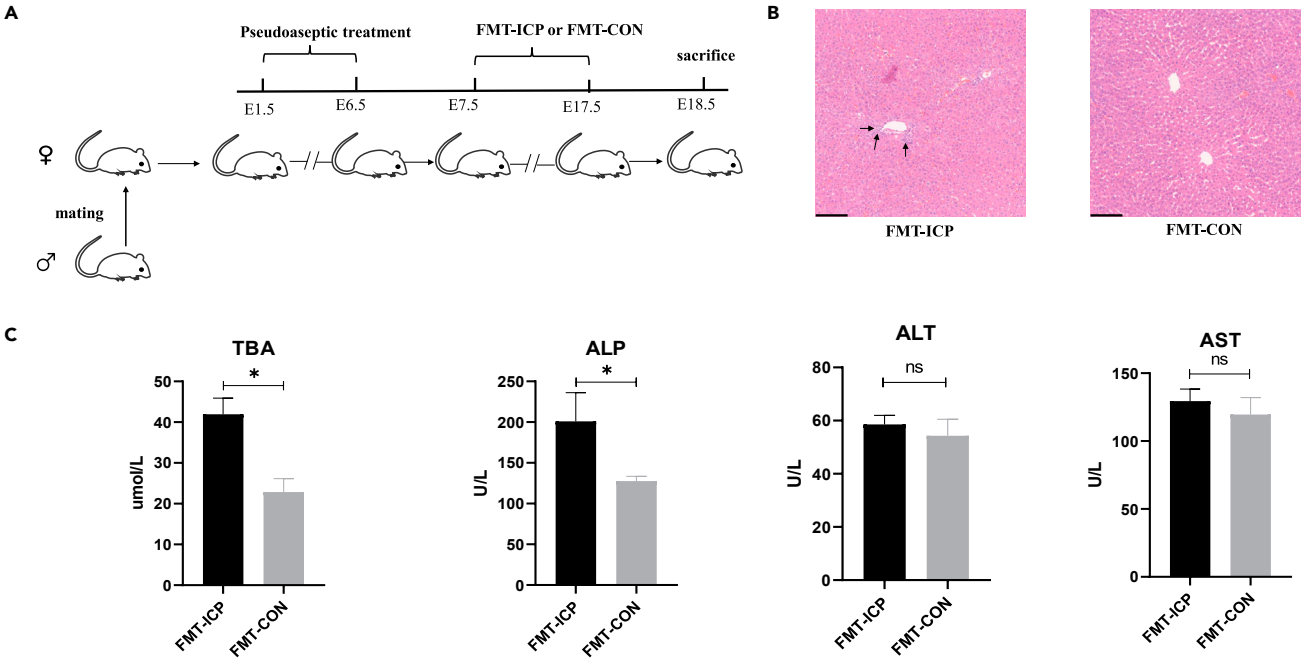

Figure 4. Changes of related indexes of liver injury in rats during pregnant after FMT

(A) An experimental design: Male and female rats were mated, and female rats were given intragastric administration of quadruple antibiotics from 1.5 to 6.5 days of pregnancy for intestinal cleaning. Feces of ICP rats and control pregnant rats collected in advance were transplanted to healthy pseudo-germfree pregnant rats respectively from 7.5 to 17.5 after pregnancy.

(B) Representative H&E staining of the liver tissues (original magnification 100×). Scale bars, 100 μm.

(C) TBA, ALP, ALT, and AST levels in the serum. Data are represented as mean ± SEM, n = 6.*p < 0.05, ns represents no statistical significance. The arrow refers to the infiltration of inflammatory cells.

of CYP7B1 and CYP27A1 (Figure S4A). Furthermore, mRNA expression of liver transporter FGFR4, SHP, and BSEP increased, while mRNA expression of NTCP decreased. mRNA expression of SHP, FXR, and FGF15 in the ileum increased (Figures 6F and 6G), and serum FGF15 levels also increased (Figure 6B). Moreover, the protein level of FXR and FGF15 also significantly increased (Figure S4B). These results demonstrate that R.I transplantation alleviated related phenotypes and improved bile acid synthesis and transport through the FXR-FGF15 signaling pathway in ICP rats.

FXR antagonist attenuated serum bile acid and liver injury in ICP rats alleviated by R.I transplantation

The aforementioned data suggested that FXR played a crucial role in alleviating bile acid synthesis and transport after R.I transplantation in ICP rats. Therefore, we hypothesize that inhibiting FXR will weaken the beneficial effects of R.I transplantation. To test this hypothesis, we transplanted the FXR inhibitor Z-Gu into ICP rats between 7.5 and 17.5 days of pregnancy (Figure 7A). The results indicated that the beneficial effects of R.I on serum bile acid and ALP in ICP rats were weakened by Z-Gu, and there was no significant difference in ALT and AST (Figure 7C). Additionally, the inhibition of FXR by Z-Gu also weakened the protective effect of R.I on hepatocytes of ICP rats (Figure 7B). Furthermore, after Z-Gu transplantation, the fecal CDCA of ICP rats decreased (Figure 7D), and there were significant differences in other types of bile acids (Figure S3C).

FXR antagonist attenuated the pathological phenotype of ICP rats remitted by R.I transplantation

Z-Gu inhibited the alleviating effect of R.I transplantation on serum endotoxin in ICP rats (Figure 8A) and also disrupted the repaired intestinal barrier function by R.I transplantation. This was evidenced by significantly lower levels of the intestinal barrier-related proteins Occludin, Claudin1, and ZO1 in Z-Gu-treated rats compared to R.I-transplanted rats (Figure 8D). Additionally, Z-Gu treatment significantly inhibited the mRNA levels of liver inflammatory factors IL-6, IL-1β, IL-10, and TNF-α that were alleviated by R.I transplantation (Figure 8C). Similarly, Z-Gu inhibited the improvement of liver Th17 and Treg by R.I transplantation (Figure 8H). As expected, Z-Gu reversed the improvement of bile acid synthesis and transport by R.I transplantation, as evidenced by increased mRNA expression of liver CYP7A1 and NTCP, decreased mRNA expression of liver FGFR4, SHP, BSEP, ileum SHP, FXR, and FGF15 (Figures 8E–8G), and increased liver CYP7A1 and CYP8B1 protein level (Figure S3C). Furthermore, serum FGF15 levels were decreased (Figure 8B) and the protein level of FXR and FGF15 also significantly decreased (Figure S4C). All of these findings suggest that Z-Gu inhibits the FXR-FGF15 signal pathway and reverses the improvement of bile acid synthesis and transport achieved by R.I transplantation.

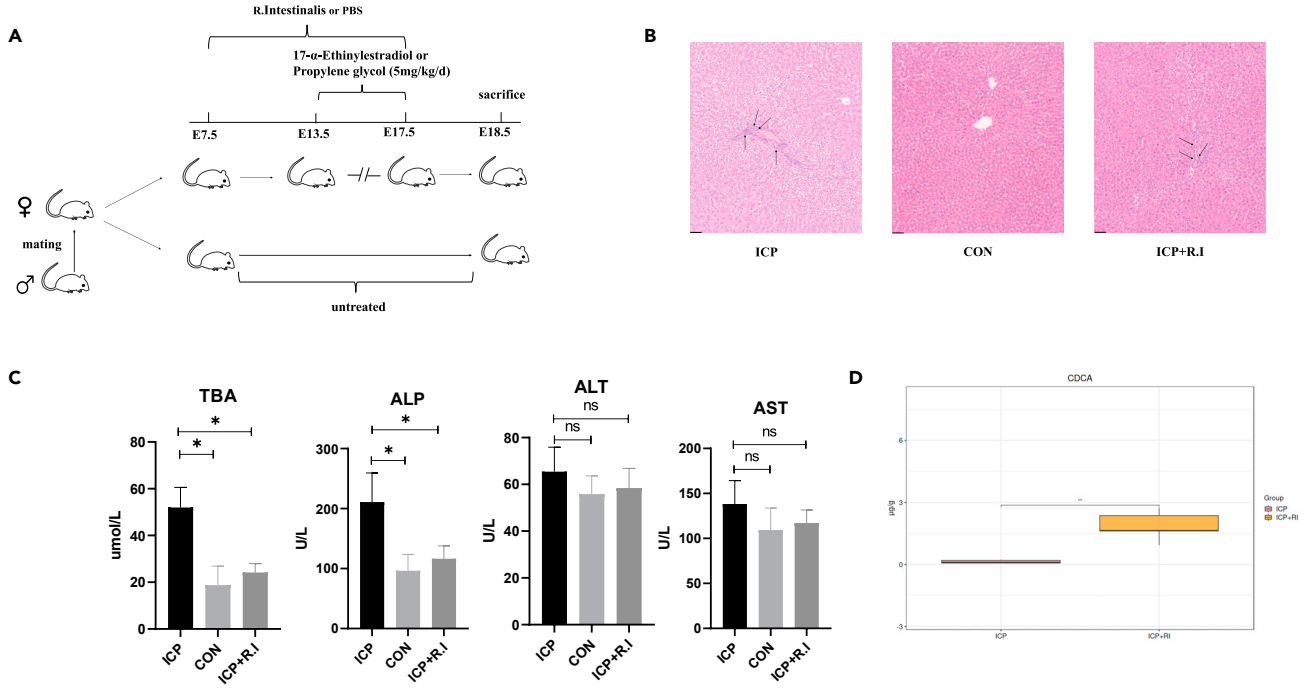

Figure 5. R.I transplantation reduced serum bile acid and alleviated liver injury in ICP rats

(A) An experimental design: Male and female rats were mated, and female rats were given intragastric administration of R.I or PBS from 7.5 to 17.5 days and injected with 17-α- ethinyl estradiol subcutaneously every day from 13.5 to 17.5 after pregnancy. Rats in the control group were not treated.

(B) Representative H&E staining of the liver tissues (original magnification 100×). Scale bars, 100 μm.

(C) TBA, ALP, ALT, and AST levels in the serum.

(D) Fecal levels of CDCA. Data are represented as mean ± SEM, n = 5–6.*p < 0.05, ns represents no statistical significance. The arrow refers to the infiltration of inflammatory cells.

DISCUSSION

Studies have indicated that there are differences in the intestinal microflora of pregnant women with ICP compared to healthy pregnant women. In clinical practice, regulating the diet of some pregnant women with ICP has been shown to alleviate their high serum bile acid levels. However, it remains unclear which intestinal microflora is associated with ICP and how changes in intestinal microflora regulate the potential mechanism of host bile acid metabolism. We conducted metagenomic sequencing and targeted bile acid testing on fecal samples from ICP rats and control group rats and found that R.I was significantly decreased and fecal CDCA was significantly decreased too. These changes were accompanied by the suppression of FXR signals. We further discovered that transplantation of R.I significantly decreased blood bile acid levels in ICP rats, improved bile acid synthesis and transport, increased fecal CDCA, increased the intestinal FXR/FGF15 signal pathway, repaired intestinal barrier function, and improved liver inflammation and immunity imbalance. Therefore, we conclude that R.I repaired ICP-related phenotypes through the bile acid/FXR-FGF15 pathway.

Firstly, we successfully established an ICP rat model and observed an increase in serum bile acid and pathological changes in the liver of these rats. Additionally, we identified abnormalities in intestinal barrier function, liver inflammation, immune imbalance, bile acid synthesis, and transporter in rats with estrogen-induced cholestasis during pregnancy. The intestinal barrier is mainly composed of closely connected intestinal cells. Tight junction proteins, such as ZO1, Claudin1, and Occludin, are essential for maintaining its integrity. When the intestinal barrier is compromised, it results in an increase in intestinal permeability. This allows pathogens or harmful substances to enter the blood-stream.[31,32] It has been suggested that activating FXR can inhibit intestinal epithelial permeability, reduce the production of inflammatory factors, and prevent chemical-induced intestinal inflammation.[33] We found that the mRNA level of FXR in the ileum of ICP rats decreased, and the fecal bile acid CDCA of ICP rats was significantly lower than that of healthy pregnant rats. CDCA has been proven to be an intestinal FXR agonist. Bile acid and intestinal flora are in a dynamic balance, and studies have shown that intestinal flora can affect the progression of the disease by altering the type or quantity of bile acid in patients.[34–36] This suggested that we can regulate the synthesis and transport of bile acid by modifying the composition of intestinal microorganisms, such as increasing the relative abundance of beneficial bacteria, to improve the high serum bile acid levels in ICP.

Through macrogenome results and correlation analysis, we speculated that R.I plays an important role in ICP. Our study further showed that transplantation of R.I decreased the serum bile acid in ICP rats, significantly decreased mRNA levels of CYP7A1, CYP8B1, and NTCP in the liver of ICP rats, increased mRNA levels of BSEP and FGF15 in the ileum and serum, and increased the concentration of CDCA in feces. This

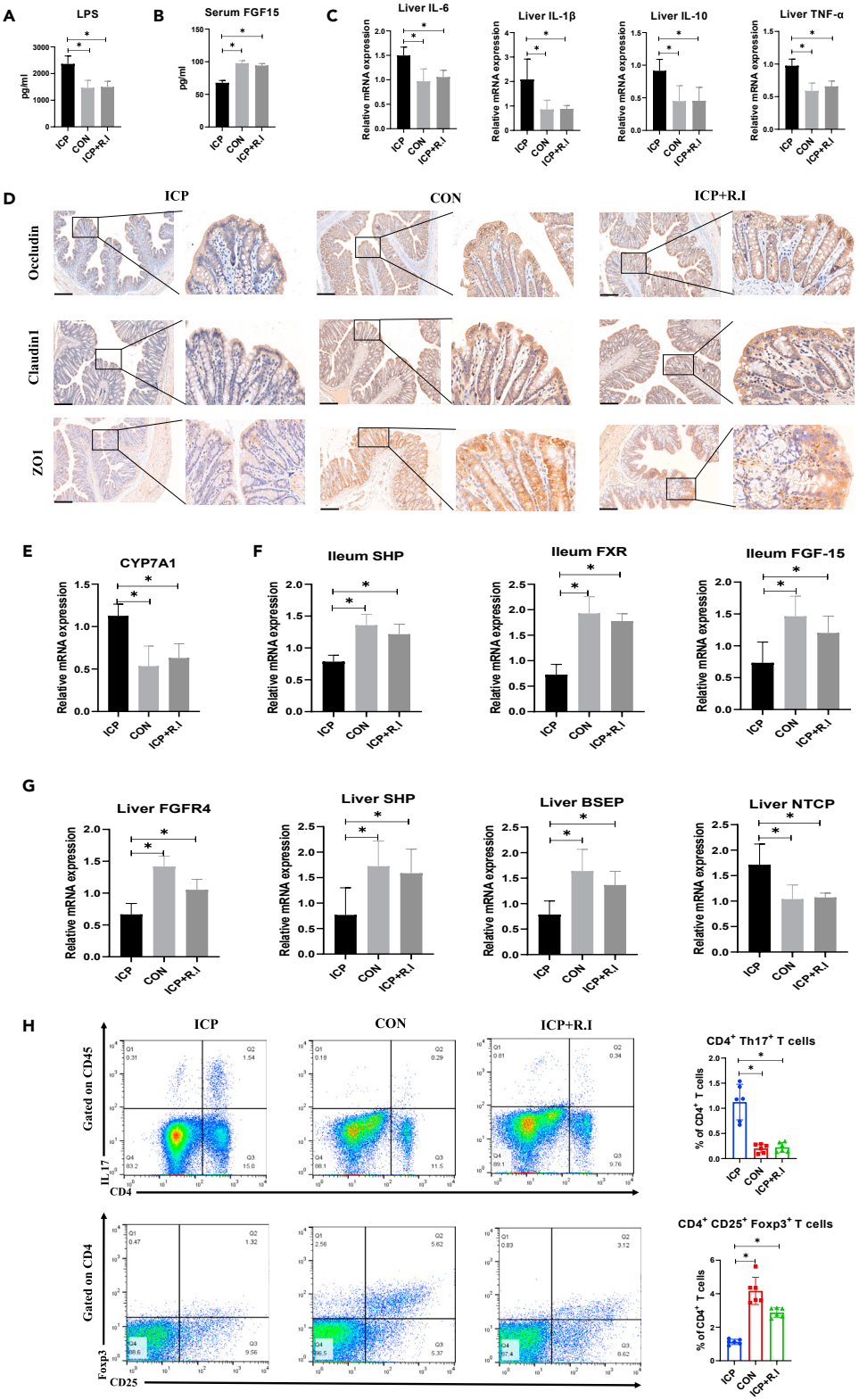

Figure 6. R.I transplantation alleviated the pathological phenotype of ICP rats

(A) Serum LPS level.

(B) Serum FGF15 level.

Figure 6. *Continued*

(C) Hepatic mRNA expression of IL-6, IL-1β, IL-10, and TNF-α.

(D) Immunohistochemistry staining for Occludin, Claudin1, and ZO1 in the colon in ICP rats and control rats was tested. The magnification is 100× and 400×, respectively. Scale bars, 100 μm.

(E) mRNA expression of CYP7A1 in the liver.

(F) mRNA expression of SHP, FXR, and FGF15 in the ileum.

(G) mRNA expression of FGFR4, SHP, BSEP, and NTCP in the liver.

(H) The representative flow cytometric plots of $CD4^+CD25^+Foxp3^+$ Treg and $CD4^+IL\text{-}17^+$ Th17 cells, respectively; and proportions of Th17 and Treg cells in each group. Data are presented as means ± SD, n = 6. *p < 0.05, CON, control group; ICP, model group.

suggested that R.I transplantation may affect bile acid synthesis and transport through bile acid/FXR-FGF15 and ultimately alleviate cholestasis. Previous studies have shown that intestinal FGF15 also affects bile acid synthesis in the liver. Bile acid binds to intestinal FXR, induces the secretion of intestinal FGF15 (human FGF-19), binds to the FGFR4 on the surface of hepatocytes, and reduces the transcription of CYP7A1 in hepatocytes, thus limiting the synthesis of bile acids.[37,38] Our research results are consistent with those reported in the literature. Inflammation and immunity are significant factors in the development of cholestasis. Studies suggested that pregnant women with ICP may have abnormal leukocyte infiltration and immune cell subset distribution in the placenta.[39,40] Our research showed that R.I transplantation effectively reduced liver inflammation and restored T cell immunity balance in ICP rats. Additionally, it decreased serum LPS levels and improved intestinal barrier function.

Previous studies have demonstrated that FXR agonists specific to the intestine can restore intestinal FXR activity and intestinal barrier integrity, regulate liver CYP7A1 and lipid metabolism, and improve bile acid/FXR-FGF15 in a mouse model of alcoholic fatty liver.[41] To demonstrate the crucial role of FXR in R.I transplantation, ICP rats were administered the FXR antagonist Z-Gu intragastrically during R.I transplantation. The results showed that the beneficial effects of R.I were counteracted by Z-Gu, leading to a decrease in the content of CDCA in

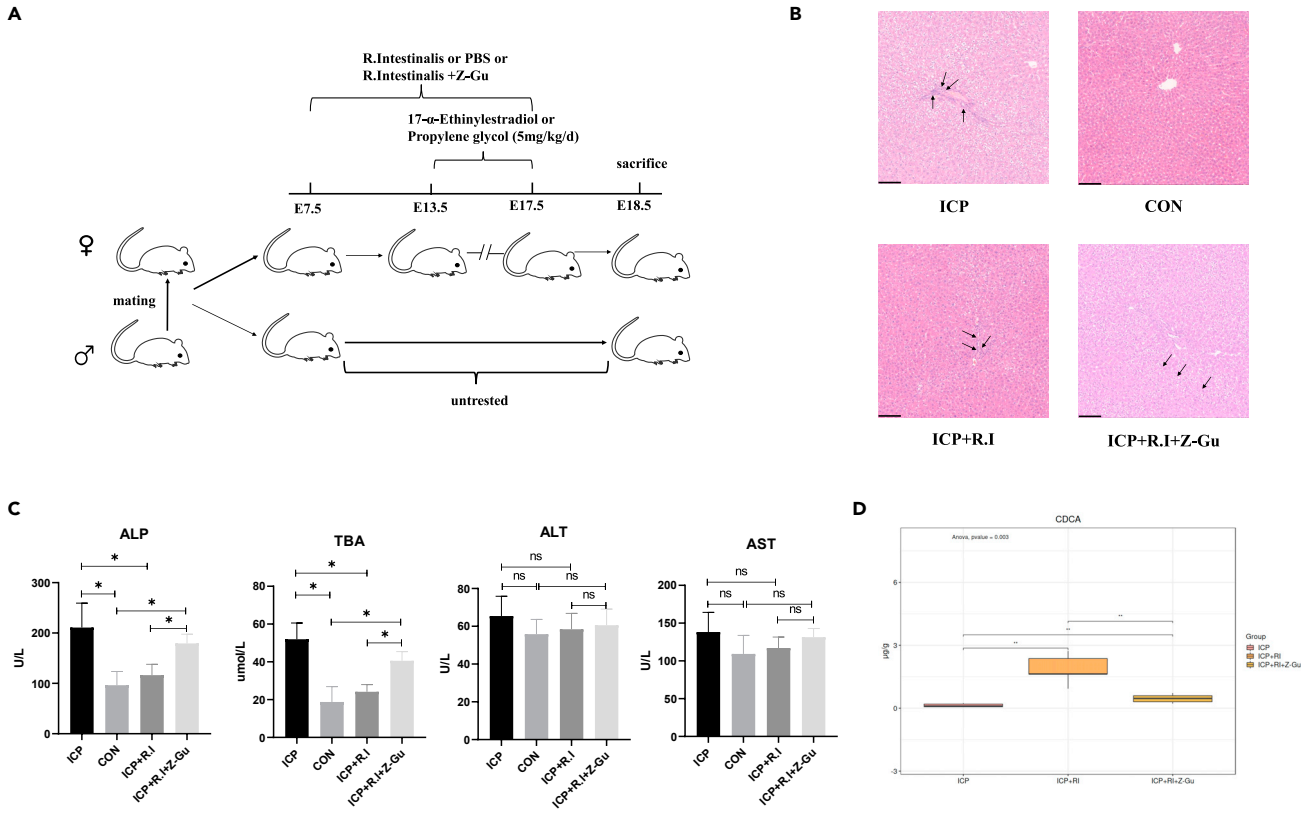

Figure 7. FXR antagonist attenuated serum bile acid and liver injury in ICP rats alleviated by R.I transplantation

(A) An experimental design: Male and female rats were mated, and female rats were given intragastric administration of R.I or PBS or R.I + Z-Gu from 7.5 to 17.5 days and injected with 17-α- ethinyl estradiol subcutaneously every day from 13.5 to 17.5 after pregnancy.

(B) Representative H&E staining of the liver tissues (original magnification 100×). Scale bars, 100 μm.

(C) TBA, ALP, ALT, and AST levels in the serum.

(D) Fecal levels of CDCA. Data are represented as mean ± SEM, n = 5–6. *p < 0.05, ns represents no statistical significance. The arrow refers to the infiltration of inflammatory cells.

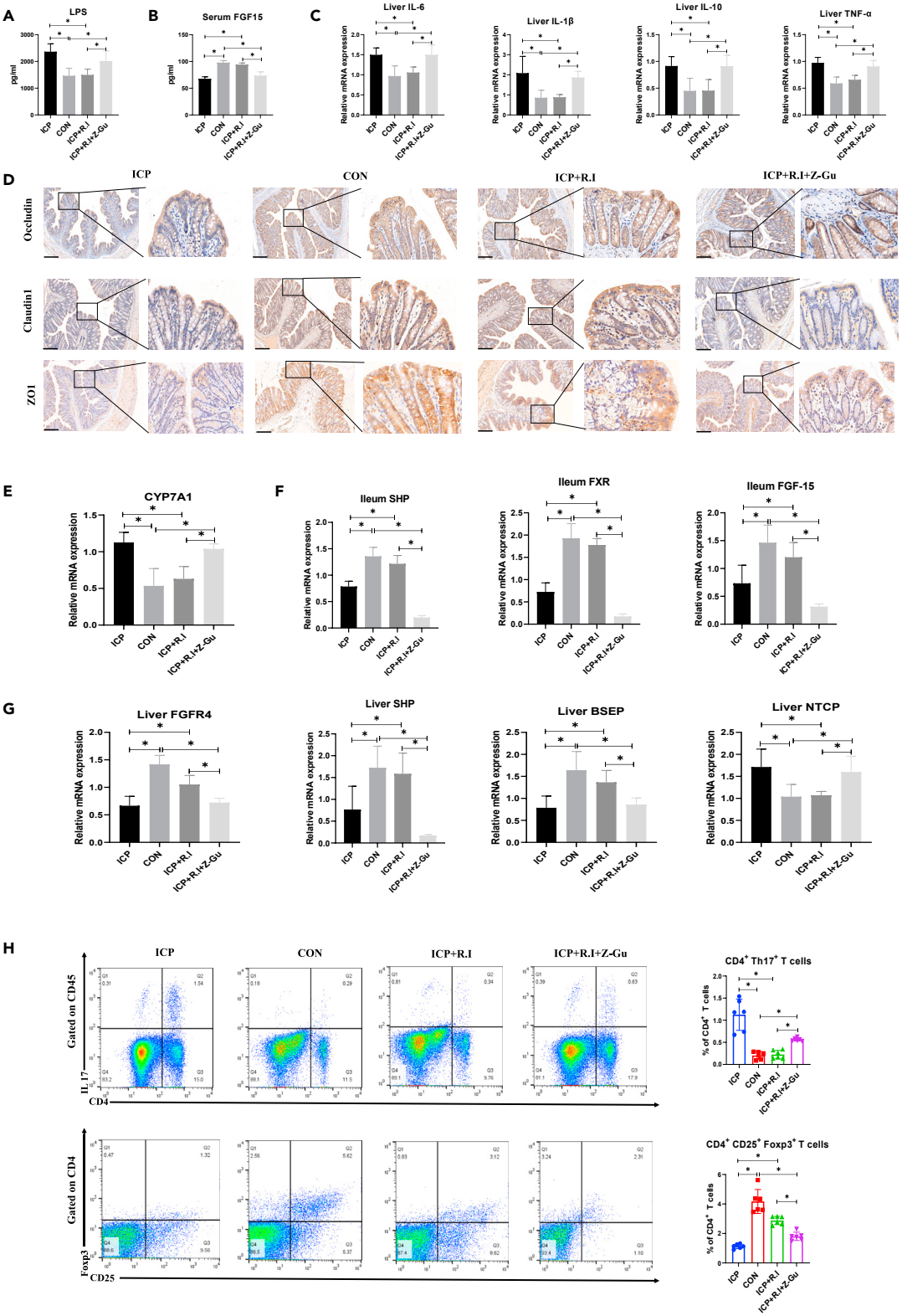

Figure 8. FXR antagonist attenuated the pathological phenotype of ICP rats remitted by R.I transplantation

(A) Serum LPS level.

(B) Serum FGF15 level.

Figure 8. *Continued*

(C) Hepatic mRNA expression of IL-6, IL-1β, IL-10, and TNF-α.

(D) Immunohistochemistry staining for Occludin, Claudin1, and ZO1 in the colon in ICP rats and control rats was tested. The magnification is 100× and 400×, respectively. Scale bars, 100 μm.

(E) mRNA expression of CYP7A1 in the liver.

(F) mRNA expression of SHP, FXR, and FGF15 in the ileum.

(G) mRNA expression of FGFR4, SHP, BSEP, and NTCP in the liver.

(H) The representative flow cytometric plots of $CD4^+CD25^+Foxp3^+$ Treg and $CD4^+IL\text{-}17^+$ Th17 cells, respectively; and proportions of Th17 and Treg cells in each group. Data are presented as means ± SD, n = 6. *p < 0.05, CON, control group; ICP, model group.

feces, a decrease in the FXR/FGF15 signal, an increase in bile acid synthesis, and a decrease in bile acid transport in the liver. Therefore, it is evident that R.I transplantation affects bile acid synthesis and transport through the bile acid/FXR-FGF15 pathway, ultimately relieving cholestasis.

In summary, our study has identified an association between intestinal flora and ICP. Estrogen-induced cholestasis during pregnancy leads to a decrease in intestinal R.I, a decrease in CDCA levels, inhibition of the FXR/FGF15 signal, an increase in bile acid synthesis, and a decrease in bile acid transport in the liver. Supplementation of R.I to ICP rats resulted in an increase in fecal CDCA levels, an increase in the FXR/FGF15 signal, a decrease in hepatic bile acid synthesis, an increase in bile acid transport, an improvement in intestinal barrier function, and an improvement in liver inflammation and immune imbalance. Furthermore, the FXR antagonist Z-Gu was found to reverse the benefits of R.I on ICP rats. This study highlights the important role of R.I in ICP and provides a new avenue for the treatment of ICP through modulation of the intestinal flora.

Limitations of the study

Our research also has some limitations. First of all, our research verifies the key role of FXR signal through FXR antagonists, but if we can further supplement FXR agonists on the basis of FXR antagonists for verification, the experimental results will be more rigorous and convincing. Secondly, R.I transplantation improved the pathological phenotype of ICP rats and activated FXR-FGF15 signaling pathway. As a new treatment method, R.I transplantation should be compared with ursodeoxycholic acid in the treatment of ICP.

STAR★METHODS

Detailed methods are provided in the online version of this paper and include the following:

- KEY RESOURCES TABLE
- RESOURCE AVAILABILITY
  - Lead contact
  - Materials availability
  - Data and code availability
- EXPERIMENTAL MODEL AND STUDY PARTICIPANT DETAILS
  - Animal experimental design
- METHOD DETAILS
  - Fecal microbiota transplantation (FMT)
  - *Roseburia intestinalis* (R.I) transplantation and Z-Guggulsterone (Z-Gu) intragastric administration
  - DNA extraction, metagenomic sequencing, and bioinformatics analysis
  - Serum biochemical value analysis
  - Enzyme-linked immunosorbent assay (ELISA)
  - Histological and immunohistochemistry analysis
  - RNA extraction and real-time PCR analysis
  - Western blotting
  - Bile acids measurements
  - Flow cytometry
- QUANTIFICATION AND STATISTICAL ANALYSIS

SUPPLEMENTAL INFORMATION

Supplemental information can be found online at https://doi.org/10.1016/j.isci.2023.108392.

ACKNOWLEDGMENTS

We express our gratitude to Mobio Biomedical Technology Co., Ltd. (Shanghai, China) for providing metagenome sequencing in this study. Additionally, we extend our appreciation to Luming Biotech Co., Ltd. (Shanghai, China) for providing targeted bile acid detection in this study. This work was supported by National Natural Science Foundation of China (grant No. 82371693), Shanghai Municipal Health Commission

(grant No. 202340113), Pudong New Area Health Committee (grant No. PW2023E-04), and Shanghai Science and Technology Commission (grant No. 20Y11907900).

AUTHOR CONTRIBUTIONS

H.S. designed and performed the experiments, analyzed the data, and drafted the manuscript. X.S. conducted the statistical analysis of the data presented in the manuscript. Y.L. and G.L. collaborated on the animal experimentation portion. Q.D. provided essential revisions to the article.

DECLARATION OF INTERESTS

The authors declare no competing interests.

Received: August 18, 2023
Revised: September 25, 2023
Accepted: November 1, 2023
Published: November 3, 2023

REFERENCES

1. Wood, A.M., Livingston, E.G., Hughes, B.L., and Kuller, J.A. (2018). Intrahepatic Cholestasis of Pregnancy: A Review of Diagnosis and Management. Obstet. Gynecol. Surv. *73*, 103–109.
2. Arrese, M., and Reyes, H. (2006). Intrahepatic cholestasis of pregnancy: a past and present riddle. Ann. Hepatol. *5*, 202–205.
3. Pillarisetty, L.S., and Sharma, A. (2023). Pregnancy Intrahepatic Cholestasis *StatPearls* Treasure Island (FL) (StatPearls Publishing LLC).
4. Mor, M., Shmueli, A., Krispin, E., Bardin, R., Sneh-Arbib, O., Braun, M., Arbib, N., and Hadar, E. (2020). Intrahepatic cholestasis of pregnancy as a risk factor for preeclampsia. Arch. Gynecol. Obstet. *301*, 655–664.
5. Glantz, A., Marschall, H.U., and Mattsson, L.A. (2004). Intrahepatic cholestasis of pregnancy: Relationships between bile acid levels and fetal complication rates. Hepatology *40*, 467–474.
6. Di Mascio, D., Quist-Nelson, J., Riegel, M., George, B., Saccone, G., Brun, R., Haslinger, C., Herrera, C., Kawakita, T., Lee, R.H., et al. (2021). Perinatal death by bile acid levels in intrahepatic cholestasis of pregnancy: a systematic review. J. Matern. Fetal Neonatal Med. *34*, 3614–3622.
7. Lozupone, C.A., Stombaugh, J.I., Gordon, J.I., Jansson, J.K., and Knight, R. (2012). Diversity, stability and resilience of the human gut microbiota. Nature *489*, 220–230.
8. Lucas, L.N., Barrett, K., Kerby, R.L., Zhang, Q., Cattaneo, L.E., Stevenson, D., Rey, F.E., and Amador-Noguez, D. (2021). Dominant Bacterial Phyla from the Human Gut Show Widespread Ability To Transform and Conjugate Bile Acids. mSystems *6*, e0080521.
9. Chiang, J.Y.L., and Ferrell, J.M. (2020). Bile acid receptors FXR and TGR5 signaling in fatty liver diseases and therapy. Am. J. Physiol. Gastrointest. Liver Physiol. *318*. G554-g573.
10. Katafuchi, T., and Makishima, M. (2022). Molecular Basis of Bile Acid-FXR-FGF15/19 Signaling Axis. Int. J. Mol. Sci. *23*, 6046.
11. Fiorucci, S., and Distrutti, E. (2015). Bile Acid-Activated Receptors, Intestinal Microbiota, and the Treatment of Metabolic Disorders. Trends Mol. Med. *21*, 702–714.
12. Hylemon, P.B., Zhou, H., Pandak, W.M., Ren, S., Gil, G., and Dent, P. (2009). Bile acids as regulatory molecules. J. Lipid Res. *50*, 1509–1520.
13. Chawla, A., Repa, J.J., Evans, R.M., and Mangelsdorf, D.J. (2001). Nuclear receptors and lipid physiology: opening the X-files. Science (New York, NY) *294*, 1866–1870.
14. Carotti, A., Marinozzi, M., Custodi, C., Cerra, B., Pellicciari, R., Gioiello, A., and Macchiarulo, A. (2014). Beyond bile acids: targeting Farnesoid X Receptor (FXR) with natural and synthetic ligands. Curr. Top. Med. Chem. *14*, 2129–2142.
15. Li, F., Jiang, C., Krausz, K.W., Li, Y., Albert, I., Hao, H., Fabre, K.M., Mitchell, J.B., Patterson, A.D., and Gonzalez, F.J. (2013). Microbiome remodelling leads to inhibition of intestinal farnesoid X receptor signalling and decreased obesity. Nat. Commun. *4*, 2384.
16. Sayin, S.I., Wahlström, A., Felin, J., Jäntti, S., Marschall, H.U., Bamberg, K., Angelin, B., Hyötyläinen, T., Orešič, M., and Bäckhed, F. (2013). Gut microbiota regulates bile acid metabolism by reducing the levels of tauro-beta-muricholic acid, a naturally occurring FXR antagonist. Cell Metab. *17*, 225–235.
17. Chiang, J.Y.L. (2009). Bile acids: regulation of synthesis. J. Lipid Res. *50*, 1955–1966.
18. Kong, B., Wang, L., Chiang, J.Y.L., Zhang, Y., Klaassen, C.D., and Guo, G.L. (2012). Mechanism of tissue-specific farnesoid X receptor in suppressing the expression of genes in bile-acid synthesis in mice. Hepatology *56*, 1034–1043.
19. Miao, J., Choi, S.E., Seok, S.M., Yang, L., Zuercher, W.J., Xu, Y., Willson, T.M., Xu, H.E., and Kemper, J.K. (2011). Ligand-dependent regulation of the activity of the orphan nuclear receptor, small heterodimer partner (SHP), in the repression of bile acid biosynthetic CYP7A1 and CYP8B1 genes. Mol. Endocrinol. *25*, 1159–1169.
20. Inagaki, T., Choi, M., Moschetta, A., Peng, L., Cummins, C.L., McDonald, J.G., Luo, G., Jones, S.A., Goodwin, B., Richardson, J.A., et al. (2005). Fibroblast growth factor 15 functions as an enterohepatic signal to regulate bile acid homeostasis. Cell Metab. *2*, 217–225.
21. Denson, L.A., Sturm, E., Echevarria, W., Zimmerman, T.L., Makishima, M., Mangelsdorf, D.J., and Karpen, S.J. (2001). The orphan nuclear receptor, shp, mediates bile acid-induced inhibition of the rat bile acid transporter, ntcp. Gastroenterology *121*, 140–147.
22. Ananthanarayanan, M., Balasubramanian, N., Makishima, M., Mangelsdorf, D.J., and Suchy, F.J. (2001). Human bile salt export pump promoter is transactivated by the farnesoid X receptor/bile acid receptor. J. Biol. Chem. *276*, 28857–28865.
23. Nie, K., Ma, K., Luo, W., Shen, Z., Yang, Z., Xiao, M., Tong, T., Yang, Y., and Wang, X. (2021). Roseburia intestinalis: A Beneficial Gut Organism From the Discoveries in Genus and Species. Front. Cell. Infect. Microbiol. *11*, 757718.
24. Hiippala, K., Jouhten, H., Ronkainen, A., Hartikainen, A., Kainulainen, V., Jalanka, J., and Satokari, R. (2018). The Potential of Gut Commensals in Reinforcing Intestinal Barrier Function and Alleviating Inflammation. Nutrients *10*, 988.
25. Zhang, C., Ma, K., Nie, K., Deng, M., Luo, W., Wu, X., Huang, Y., and Wang, X. (2022). Assessment of the safety and probiotic properties of Roseburia intestinalis: A potential "Next Generation Probiotic". Front. Microbiol. *13*, 973046.
26. Shen, Z., Luo, W., Tan, B., Nie, K., Deng, M., Wu, S., Xiao, M., Wu, X., Meng, X., Tong, T., et al. (2022). Roseburia intestinalis stimulates TLR5-dependent intestinal immunity against Crohn's disease. EBioMedicine *85*, 104285.
27. Seo, B., Jeon, K., Moon, S., Lee, K., Kim, W.K., Jeong, H., Cha, K.H., Lim, M.Y., Kang, W., Kweon, M.N., et al. (2020). Roseburia spp. Abundance Associates with Alcohol Consumption in Humans and Its Administration Ameliorates Alcoholic Fatty Liver in Mice. Cell host & microbe *27*, 25–40.e6.
28. Zhan, Q., Qi, X., Weng, R., Xi, F., Chen, Y., Wang, Y., Hu, W., Zhao, B., and Luo, Q. (2021). Alterations of the Human Gut Microbiota in Intrahepatic Cholestasis of Pregnancy. Front. Cell. Infect. Microbiol. *11*, 635680.
29. Ren, S., Zhou, Y., and Xuan, R. (2021). Research progress in the role of gut microbiota and its metabolites in intrahepatic cholestasis of pregnancy. Expert Rev. Gastroenterol. Hepatol. *15*, 1361–1366.
30. Li, G.H., Huang, S.J., Li, X., Liu, X.S., and Du, Q.L. (2020). Response of gut microbiota to serum metabolome changes in intrahepatic

cholestasis of pregnant patients. World J. Gastroenterol. *26*, 7338–7351.

31. Arrieta, M.C., Bistritz, L., and Meddings, J.B. (2006). Alterations in intestinal permeability. Gut *55*, 1512–1520.
32. Milosevic, I., Vujovic, A., Barac, A., Djelic, M., Korac, M., Radovanovic Spurnic, A., Gmizic, I., Stevanovic, O., Djordjevic, V., Lekic, N., et al. (2019). Gut-Liver Axis, Gut Microbiota, and Its Modulation in the Management of Liver Diseases: A Review of the Literature. Int. J. Mol. Sci. *20*, 395.
33. Gadaleta, R.M., van Erpecum, K.J., Oldenburg, B., Willemsen, E.C.L., Renooij, W., Murzilli, S., Klomp, L.W.J., Siersema, P.D., Schipper, M.E.I., Danese, S., et al. (2011). Farnesoid X receptor activation inhibits inflammation and preserves the intestinal barrier in inflammatory bowel disease. Gut *60*, 463–472.
34. Makishima, M., Okamoto, A.Y., Repa, J.J., Tu, H., Learned, R.M., Luk, A., Hull, M.V., Lustig, K.D., Mangelsdorf, D.J., and Shan, B. (1999). Identification of a nuclear receptor for bile acids. Science (New York, NY) *284*, 1362–1365.
35. Parks, D.J., Blanchard, S.G., Bledsoe, R.K., Chandra, G., Consler, T.G., Kliewer, S.A., Stimmel, J.B., Willson, T.M., Zavacki, A.M., Moore, D.D., and Lehmann, J.M. (1999). Bile acids: natural ligands for an orphan nuclear receptor. Science (New York, NY) *284*, 1365–1368.
36. Wang, H., Chen, J., Hollister, K., Sowers, L.C., and Forman, B.M. (1999). Endogenous bile acids are ligands for the nuclear receptor FXR/BAR. Mol. Cell *3*, 543–553.
37. Dawson, P.A., and Karpen, S.J. (2015). Intestinal transport and metabolism of bile acids. J. Lipid Res. *56*, 1085–1099.
38. Schaap, F.G., Trauner, M., and Jansen, P.L.M. (2014). Bile acid receptors as targets for drug development. Nat. Rev. Gastroenterol. Hepatol. *11*, 55–67.
39. Kong, X., Kong, Y., Zhang, F., Wang, T., and Zhu, X. (2018). Expression and significance of dendritic cells and Th17/Treg in serum and placental tissues of patients with intrahepatic cholestasis of pregnancy. J. Matern. Fetal Neonatal Med. *31*, 901–906.
40. Zhang, Y., Huang, X., Zhou, J., Yin, Y., Zhang, T., and Chen, D. (2018). PPARγ provides anti-inflammatory and protective effects in intrahepatic cholestasis of pregnancy through NF-κB pathway. Biochem. Biophys. Res. Commun. *504*, 834–842.
41. Hartmann, P., Hochrath, K., Horvath, A., Chen, P., Seebauer, C.T., Llorente, C., Wang, L., Alnouti, Y., Fouts, D.E., Stärkel, P., et al. (2018). Modulation of the intestinal bile acid/farnesoid X receptor/fibroblast growth factor 15 axis improves alcoholic liver disease in mice. Hepatology *67*, 2150–2166.

STAR★METHODS

KEY RESOURCES TABLE

REAGENT or RESOURCE	SOURCE	IDENTIFIER
Antibodies		
CYP7A1	ABclonal	Cat# A10615; RRID: AB_2758151
CYP8B1	ABclonal	Cat# A22538; RRID: AB_3073910
FXR	ABclonal	Cat# A12788; RRID: AB_2759628
Occludin	Servicebio Co., Ltd	Cat# GB111401; RRID: AB_2938979
FGF-15	ABCAM	Cat# AB229630; RRID: AB_3073912
ZO1	ABCAM	Cat# AB221547; RRID: AB_2892660
Claudin1	Proteintech	Cat# 13050-1-AP; RRID: AB_2079881
Critical commercial assays		
LPS ELISA kit	Wellbio Technology Co., Ltd	ER9262M
FGF-15 ELISA kit	Wellbio Technology Co., Ltd	ER20170
Genious 2X SYBR Green Fast qPCR Mix	ABclonal	RK21206
Deposited data		
Sequencing Data	This paper	Sequence Read Archive (SRA) database with reference number PRJNA1002065 and Genome Sequence Archive (GSA) database with reference number OMIX004988
Software and algorithms		
GraphPad Prism	GraphPad Prism	https://www.graphpad.com/
ImageJ	ImageJ	https://imagej.nih.gov/ij/
FlowJo	FlowJo	https://www.flowjo.com/
Other		
17-α-ethinylestradiol	TargetMol	T1424
(±)-1,2-Propanediol	MedChemExpress	HY-Y0921
Z-Guggulsterone	TargetMol	T17280

RESOURCE AVAILABILITY

Lead contact

Further information and requests for resources and reagents should be directed to and will be fulfilled by the lead contact, Qiaoling Du: (19921781186@139.com).

Materials availability

This study did not generate new unique reagents.

Data and code availability

The raw data that support the findings of this study are openly available in the Sequence Read Archive (SRA) database with reference number PRJNA1002065and Genome Sequence Archive (GSA) database with reference number OMIX004988.

This paper does not report original code.

Any additional information required to reanalyze the data reported in this paper is available from the lead contact upon request.

EXPERIMENTAL MODEL AND STUDY PARTICIPANT DETAILS

Animal experimental design

The animal experiment protocol was approved by the Science and Technology Ethics Committee of Tongji University. Female and male Sprague Dawley (SD) rats, at eight weeks old, were obtained from WeiTongLiHua (Beijing, China). After two weeks of adaptation to a specific

pathogen-free (SPF) environment, female and male SD rats were housed together in the same cage during estrus. Successful mating was confirmed by the presence of milky white or yellowish vaginal plugs upon vaginal swab examination or by the observation of sperm under a microscope after vaginal smear, and was recorded as day 0.5 of pregnancy. In the ICP rat model experiment, 17-α-ethinylestradiol (5 mg/kg, TargetMol, USA) was dissolved in (±)-1,2-Propanediol (MedChemExpress (Monmouth Junction, NJ, USA)) and 0.5 mL/100g was subcutaneously injected at the back of the rats' neck on days 13.5–17.5 of pregnancy. Rats in the control group were subcutaneously injected with 0.5 mL/100g (±)-1,2-Propanediol. Blood samples from the orbital vein and feces were collected from SD rats at 18.5 days of gestation.

METHOD DETAILS

Antibodies against CYP7A1, CYP8B1, and FXR used for Western Blotting were purchased from ABclonal (A10615, A22538, A12788, Wuhan, China). Antibodies against Occludin used for Immunohistochemistry were purchased from Servicebio Co., Ltd (GB111401, Wuhan, China). Antibodies against FGF-15 used for Western Blotting were purchased from ABCAM (AB229630, Cambridge, MA). Antibodies against ZO1 used for Immunohistochemistry were purchased from ABCAM (AB221547, Cambridge, MA). Antibodies against Claudin1 used for Immunohistochemistry were purchased from Proteintech (13050-1-AP, USA). LPS and FGF-15 ELISA kits were purchased from Wellbio Technology Co., Ltd (ER9262M, ER20170, Shanghai, China). Z-Guggulsterone was purchased from Topscience. Reagents used for Real-time PCR were purchased from ABclonal (RK21206, Wuhan, China). Reagents used for Immunohistochemistry (except for antibodies) were purchased from Wellbio Technology Co., Ltd (Sodium citrate antigen repair solution (50x), WH1032; Endogenous peroxidase blocker-paraffin tablets, WH1028; EDTA antigen repair solution (50x), WH1034; Rabbit—SABC kit, WH1057; DAB chromogenic kit 20x, WB0167).

Fecal microbiota transplantation (FMT)

The feces of both ICP rats and healthy pregnant rats were collected in advance and stored in a freezer at −80°C. Female rats were treated with quadruple antibiotics from 1.5 to 6.5 days of pregnancy, and the pseudo-germfree pregnant rats were randomly divided into two groups. The antibiotic solution was freshly prepared daily and wrapped in tin foil to avoid exposure to light. The specific ingredients were as follows: the concentration of ampicillin sodium, neomycin sulfate, and metronidazole was 1 mg/ml, and the concentration of vancomycin hydrochloride was 0.5 mg/ml. Each rat was intragastrically fed with 2mL of the solution every day. 1 gram of feces was dissolved in 5mL of phosphate buffer solution (PBS), suspended for 5 min by vortex, and then filtered out the impurities in the feces with sterile gauze. The dosage of transplantation was 2mL per rat every day. The feces collected in advance from ICP model rats were transplanted to healthy pseudo-germfree pregnant rats (marked as FMT-ICP), and the feces collected in advance from healthy pregnant rats were transferred to healthy pseudo-germfree pregnant rats (marked as FMT-CON). The transplantation was performed between 7.5 and 17.5 days of pregnancy.

Roseburia intestinalis (R.I) transplantation and Z-Guggulsterone (Z-Gu) intragastric administration

Our experiment was divided into four groups: (A) Control (CON) group, (B) ICP group, (C) ICP+ R.I group, and (D) ICP+ R.I + Z-Gu group. We purchased *Roseburia intestinalis* from Ningbo Mingzhou Biotechnology Co., Ltd., with a concentration of $1 * 10^9$ colony forming units (CFU)/mL. Each rat was administered 2 mL of bacterial liquid by gavage every day for 11 days. In the R.I transplantation experiment, rats in groups A and B were given the same volume of PBS solution, while rats in group D were given intragastric administration of the FXR inhibitor Z-Gu at a dose of 10 mg/kg.

DNA extraction, metagenomic sequencing, and bioinformatics analysis

Genomic DNA was extracted from each sample by using E.Z.N.A. Stool DNA Kit (Omega Bio-tek, Inc., GA) and then fragmented (~350 bp, SCIENTZ08-III). The DNA library was constructed according to the instructions of the Hieff NGS Ultima Pro DNA Library Prep Kit for Illumina V2 (Yeasen Biotechnology Co., Ltd., Shanghai), bridge PCR and sequencing was performed on the NovaSeq 6000 platform (Illumina Inc., USA). The software knead-data was used to perform quality control on the raw reads and obtain high-quality reads for each sample. The reads were assembled and genes were predicted using Megahit and Prodigal, and a non-redundant gene set was constructed using CD-HIT and Salmon software, and the gene abundance in each sample was calculated. The non-redundant gene set was blasted against the NR database and eggNOG database to gain the taxonomic and functional annotations by using the software DIAMOND, the COG, KEGG orthologs (KO), Pathway, Module, CAZy, CARD, and VFDB information corresponding to the genes was obtained. The alpha diversity was used to analyze the richness and diversity (ACE index, Chao Index, Shannon Index, and Simpson Index) of intestinal flora. Principal coordinate analysis (PCoA) based on Bray-Curtis and Jaccard-Binary distances was used to display the difference in community structure between groups. Permutation multivariate analysis of variance (PerMANOVA, also known as Adonis analysis) was used to test the statistical significance of differences between groups. R software was used to generate a bar chart of the bacterial composition in each sample from the phylum level to the species level, and the relative abundance of bacterial taxa between groups was analyzed using non-parametric Mann-Whitney U test, with $p < 0.05$ indicating significant differences. The linear discriminant analysis effect size (LEfSe) was used to identify key taxa that differed between groups at the phylum to species levels. Functional groups (KO, KEGG pathway, CAZy, CARD, VFDB, etc.) that differed between groups were identified using LEfSe analysis.

Serum biochemical value analysis

The serum samples were centrifuged at 4000 rpm for 10 min, and the supernatant was collected. An automatic biochemical analyzer (Chemray 800, Leidu Life Technology, Shenzhen) was used to examine four indices: glutamic-pyruvic transaminase, glutamic oxaloacetic transaminase, alkaline phosphatase, and total bile acid.

Enzyme-linked immunosorbent assay (ELISA)

Serum levels of lipopolysaccharide (LPS) and fibroblast growth factor 15 (FGF-15) were assessed following the manufacturer's instructions (Wellbio Technology Co., Ltd, Shanghai, China). All samples and standard curve reagents were measured in triplicate.

Histological and immunohistochemistry analysis

The fresh liver and colon tissue from rats were placed in a 10% formalin fixation solution. The samples were then dehydrated using varying concentrations of ethanol, immersed in xylene, and embedded in paraffin. Each slice was cut into 5 μm thin sections using a paraffin slicer and stained with hematoxylin-eosin (HE) to observe any pathological changes in the liver. For immunohistochemistry, all reagents were purchased from Wellbio Technology Co., Ltd (Claudin1(1:200; 13050-1-AP; Proteintech), ZO1(1:500; AB221547; ABCAM), Occludin (1:500; GB111401; Servicebio)). First, the paraffin slices were baked in an oven, dewaxed with xylene, hydrated with varying concentrations of ethanol, and subjected to thermal antigen repair. Antibodies were then added to the slices and left overnight in a refrigerator at 4°C. On the second day, biotin goat anti-rabbit IgG and chromogenic agents were added respectively. The slices were then slightly re-stained with hematoxylin, dehydrated, sealed, and finally observed under a microscope.

RNA extraction and real-time PCR analysis

To extract RNA, 1mL of Trizol was added to 100mg of liver and ileum tissue. After grinding, 200μL of chloroform was added, shaken, and mixed for 15 s. The mixture was then centrifuged at 12000r at 4°C for 15 min. The liquid from the upper layer was collected and the same volume of isopropanol was added. The mixture was centrifuged at 12000r at 4°C for 10 min. After discarding the upper liquid, 1mL of 75% ethanol was added to wash the RNA 3 times. Finally, all the liquid was discarded, and 20μL of diethylpyrocarbonate (DEPC) water was added after natural drying. The RNA concentration was measured. For reverse transcription, all samples were converted into complementary DNA (cDNA) using the reverse transcribed protocol (ABclonal, RK20428, Wuhan, China). The primers for this study were purchased from Tsingke Biotechnology Co., Ltd. (Beijing, China). For quantitative Polymerase Chain Reaction (qPCR), a reaction solution was prepared using 10μL as the system, Genious 2X SYBR Green Fast qPCR Mix (Low ROX Premixed) 5μL, Forward Primer 0.2μL, Reverse Primer 0.2μL, cDNA 1μL, and double distilled water (ddH_2O) 3.6μL. The qPCR reaction program was set up according to the protocol (ABclonal, RK21206, Wuhan, China), and the biological system 7500 fast real-time PCR system (Thermo Fisher Science, Waltham, MA, USA) was used for quantitative real-time PCR (qRT-PCR). Glyceraldehyde 3-phosphate dehydrogenase was used as the standard control, and the primer sequence is shown in Table S1. The relative quantification of gene expression was carried out by the $2^{-\Delta\Delta CT}$ method.

Western blotting

After extracting tissue proteins, the protein concentration was determined using the bicinchoninic acid (BCA) protein analysis kit (WB6501, New Cell & Molecular Biotech). An equal amount of protein (20 μg/lane) was added to each lane, separated by sodium dodecyl sulfate-polyacrylamide gel electrophoresis, and then transferred to a polyvinylidene fluoride membrane (PVDF membrane, EMD Millipore, Burlington, MA, USA). The PVDF membrane was immersed in Tris-buffered saline with Tween (TBST) containing skim milk, incubated on a shaker for 1.5 h, and then left overnight with GAPDH (1:10000; AB2100; New Cell & Molecular Biotech), CYP7A1 (1:1000; A10615; ABclonal), CYP8B1 (1:200; A22538; ABclonal), FXR (1:500; A12788; ABclonal), and FGF15 (1:2000; AB229630; ABCAM) in a refrigerator at 4°C. The membrane was then incubated with goat anti-rabbit IgG(H + L) labeled with horseradish peroxidase (1:1000; A0208; Beyotime) or goat anti-mouse IgG(H + L) labeled with horseradish peroxidase (1:1000; A0216; Beyotime) for 1 h at room temperature. The image was captured using a chemiluminescence imaging system (Shanghai Taineng Technology Co., Ltd., China). The intensity of protein bands was quantified using ImageJ2 software (National Institutes of Health, Bethesda, Maryland, USA).

Bile acids measurements

All chemicals and solvents used in this study were of analytical or high-performance liquid chromatography (HPLC) grade. Water, methanol, acetonitrile, 2-propanol, and formic acid were procured from Thermo Fisher Scientific (Waltham, MA, USA).

The feces of ICP pregnant rats and healthy pregnant rats at 18.5 days of pregnancy were collected. Weigh 30mg of sample, add 100ul of precooled methanol-water solution (1: 1, V/V), including isotope internal standard cholic acid-2,2,4,4-d4 and glycocholic acid-(glycine -1-13C)) solution, then put two steel balls into the mixture and grind it with a grinder (60Hz, 2min). After grinding, add 500ul of precooled acetonitrile (5% ammonia water, V/V). The whole sample was ultrasonically extracted in an ice-water bath for 20min, stand for 30 min at −20°C, then centrifuged for 10 min (4°C, 13000rpm), and 300ul of supernatant was taken. The supernatant was dried by nitrogen flow, and the dried sample was dissolved again with precooled 300ul methanol-water (1: 1, V/V), and ultrasonic was performed for 5 min. Centrifuge again under the same conditions, take 200ul of supernatant, filter with a 0.22 μm m organic phase pinhole filter, transfer to the brown injection bottle, and store it at −80°C for UPLC-MS/MS analysis. Quality control samples (QC) are prepared by mixing the extracts of all samples in equal volumes. In this

experiment, a Nexera UPLC LC-30A(SHIMADZU) liquid chromatography, a Phenomenex Kinetex C18 (2.1 mm × 100 mm, 2.6 μm) chromatographic column, and an AB Sciex Qtrap 5500 mass spectrometer were used for analysis. Using water (1% formic acid) and methanol-acetonitrile-isopropanol (1: 1: 1, V/V, 1% formic acid) as mobile phases, gradient elution was performed. Electrospray ionization (ESI) is used in both positive and negative modes, with a negative ion spraying voltage of −4,500 V and a positive ion spraying voltage of 5500 V. Targeted metabolites were analyzed in multiple reaction monitoring (MRM) modes. The MRM pairs, declustering potentials (DP), and collision energies (CE) were optimized for each analyte. Data acquisitions and further analysis were conducted using Analyst software. SCIEX OS-MQ software was used to quantify all metabolites. The standard sample was accurately weighed and dissolved in methanol to prepare a mixed standard solution. Then the standard solution was diluted in gradient and the standard curve equation of different metabolites was calculated by linear regression according to the peak area of the mass spectrum of different concentrations of standard samples (0.04ng/mL-100 ng/ml). The peak area of the metabolite was brought into the regression equation fitted by the standard curve, and the concentration of the metabolite was obtained.

Flow cytometry

The liver of rats was prepared as a single-cell suspension. For Treg cells, surface staining was performed using CD4 and CD25 antibodies, followed by nuclear staining using forkhead box protein 3 (Foxp3) antibodies. For Th17 cells, after stimulation with a stimulant, the cells were incubated in a carbon dioxide incubator for 5 h. Then, CD4 and CD25 antibodies were added, followed by cytostaining and IL-17 antibodies. All antibodies were purchased from Biolegend and eBioscience (CD4 (PE/Cyanine, Biolegend, 201515); CD25 (PE, Biolegend, 202105); CD45 (FITC, Biolegend, 202205); Foxp3 (Alexa Fluor 647; Biolegend; 320013); IL17 (APC; eBioscience; 17-7177-81)). The stained cells were analyzed using flow cytometry (BD, FACSCalibur) and FLOWJO 10.8.1 software (Becton, Dickinson & Company, USA).

QUANTIFICATION AND STATISTICAL ANALYSIS

The data were presented as means ± standard error of the mean (SEM) and analyzed using GraphPad Prism 8.0 software. The Student's t-test was used for comparisons between two groups, while one-way analysis of variance (ANOVA) was used for comparisons between three or more groups. A p-value of less than 0.05 was considered statistically significant. Additional materials, methods, and figures can be found in the supplemental information.